



Article

BIOCOMPATIBILITY EVALUATION AND ENHANCEMENT OF ELASTOMERIC COATINGS MADE USING TABLE-TOP OPTICAL 3D PRINTER

Giedrė Grigalevičiūtė ¹, Daiva Baltriukienė ² , Virginija Bukelskienė ², and
Mangirdas Malinauskas ^{1,*} 

¹ Vilnius University, Faculty of Physics, Laser Research Center, Vilnius, Lithuania

² Vilnius University, Faculty of Biochemistry, Life Sciences Center, Vilnius, Lithuania

* Correspondence: mangirdas.malinauskas@ff.vu.lt; Tel.: +37060002843

Abstract: In this experimental report the biocompatibility of elastomeric scaffold structures made *via* stereolithography employing table-top 3D printer Ember (*Autodesk*) and commercial resin FormLabs Flexible (FormLabs) was studied. The samples were manufactured using standard printing and development protocol, which is known to inherit cytotoxicity due to remaining non-polymerized remaining monomers, despite the polymerized material being fully biocompatible. Additional steps were taken to remedy this problem: the fabricated structures were soaked in isopropanol and methanol for different conditions (temperature, duration) in order to leach out the non-polymerized monomers. Also disc-shaped 3D-printed structures were UV exposed to assure maximum polymerization degree of the material. Post-processed structures were seeded with myogenic stem cells and the number of live cells was evaluated as an indicator for the material biocompatibility. The straightforward post-processing protocol enhances the biocompatibility of the surfaces by 7 times after 7 days soaking in isopropanol and methanol and is comparable to control (glass and polystyrene) samples. This proposes the approach as a novel and simple method to be widely applicable for dramatic cytotoxicity reduction of optically 3D printed micro-/nano-scaffolds for a wide range of biomedical studies and applications.

Keywords: Stereolithography; Elastomer; Biocompatibility; Post-processing; UV curing; Thermal treatment; Optical 3D printing

1. Introduction

Recently diverse 3D printing technologies have received a lot of attention in the areas of science and industry [1]. Differently from traditional processes of manufacturing, 3D printing allows computer aided manufacturing (CAM) of arbitrary geometry objects using computer aided design (CAD) models out of variety of materials with minimal fabrication costs. It can be applied in various fields such as mass-customized production [2], prototyping and dentistry [3]. One of the most promising is regenerative medicine, where 3D printed objects have already made a great influence in such areas as orthopedics [4], face and skull reconstruction [5], plastic, teeth and mouth surgeries [6], etc. Another 3D printing application area in medicine is tissue engineering [7]. For this purpose, cells can be seeded into well-defined geometry 3D printed structures [8–10] and artificial tissue or organ can be grown and implanted into a living organism [8,11].

A broad range of biomaterials depending on their chemical structure, mechanical and biological properties are used in 3D printing [12,13]. However, there is still a lack of elastomeric photostructurable resins that would fit for tissue engineering requirements for scaffolds [7,14]. This significantly

influences a demand to synthesize novel biopolymers with tunable bio-properties (mechanical, wetting, bioresorptive, etc). On the other hand, the optimizing procedure of the biocompatibility of existing commercial resins could also significantly contribute to the wide-spread of the technique in advanced clinics [15]. It was shown that cell viability can be increased by higher polymerization degree or monomer-to-polymer conversion level [16]. For this reason, additional UV exposure after polymerization could be a solution in order to optimize biocompatibility. There is also shown that prolonged soaking of polymerized structures results in better cell viability because of leaching out of monomers toxic for cell [17]. However, in these reports biocompatibility optimization protocol was not defined as the research was not systematic.

Here, we report a straightforward procedure for optimization the biocompatibility of 3D printed structures using both commercially available optical 3D printer and widespread resin. The protocol includes simple additional soaking in methanol and isopropanol under different conditions in sequence to extra UV exposure. The achieved improvement in biocompatibility significantly reaches up to 7 times and is comparable to glass/polystyrene known as biocompatible reference materials.

2. Materials and Methods

During the experiments 3D printer *Autodesk Ember*, which provides projection stereolithography based on digital mirror device shaping the light source of 405 nm wavelength and 5W power layer-by-layer, was used. Disk-structures were fabricated out of commercial *Formlabs Flexible* photoresin, which consists of acrylate monomers and oligomers and owns elastomeric properties [18]. Several default printing parameters were changed for the *Formlabs Flexible* processing: layer height - 0,025 mm, wait (before exposure) - 6 s, exposure time - 14 s, separation velocities - 1rpm. The disk-shaped structures of 13 mm diameter were polymerized and post-processed in order to test biocompatibility (Figure 1). Additional UV exposition (using Thorlabs CS2010 UV LED lamp, wavelength 365 nm, power 270 mW) in two different durations of 1 hour and 22 hours was implemented in order to increase polymerization degree [19]. Also, leaching out the not polymerized monomers that are toxic for cells [17] was carried out when soaking fabricated structures in isopropyl alcohol and methanol in two different temperatures (22 – 25°C and 37 – 40°C) and different durations - from 1 day to 8 days. Experiment plan is shown in Figure 2.

The viability of cells was determined using the standard MTT [3-(4,5-dimethylthiazol-2-yl)-2,5-diphenyltetrazolium bromide] assay. Myogenic stem cells were seeded on samples at a density of 30,000 cells/mL/sample, using glass slides as control. The samples were placed in 24-well polystyrene tissue culture plates and incubated at 37 °C with 5 % CO₂ atmosphere. After 24 h of culture, the medium was discarded and the samples were treated with MTT (1 mg/mL) and incubated for 1 h at 37°C. The MTT solution was then carefully replaced with 200 µL of DMSO to solubilize the formazan and subsequently, 100 µL of the formazan-DMSO solution was used to measure absorption. The optical density at 545 nm was measured by using an automatic microplate reader Varioskan Flash (Thermo Scientific). Results were calculated as a ratio between cells grown on tested materials and polystyrene tissue culture plate surface.

To assess the mode of cell death, myogenic stem cells were seeded on samples at a density of 50,000 cells/mL/sample. The samples were then incubated at 37°C with 5% CO₂ atmosphere. After being cultured for 24 h, cells were trypsinized (0.25 % trypsin). 25 µL of cell suspensions were transferred to glass slides. Dual fluorescent staining solution (2 µL) containing 100 µg/ml acridine orange and 100 µg/ml ethidium bromide (AO/EB, Sigma, St. Louis, MO) was added to each suspension and then covered with a coverslip. The morphology of apoptotic cells was examined and 100 cells were counted using a fluorescent microscope (OLYMPUS, Japan). Acridine orange was used to characterize chromatin condensation and segmentation; ethidium bromide was used to characterize membrane integrity as described in [20]. Cells were categorized as follows: viable, viable apoptotic, nonviable apoptotic and necrotic.

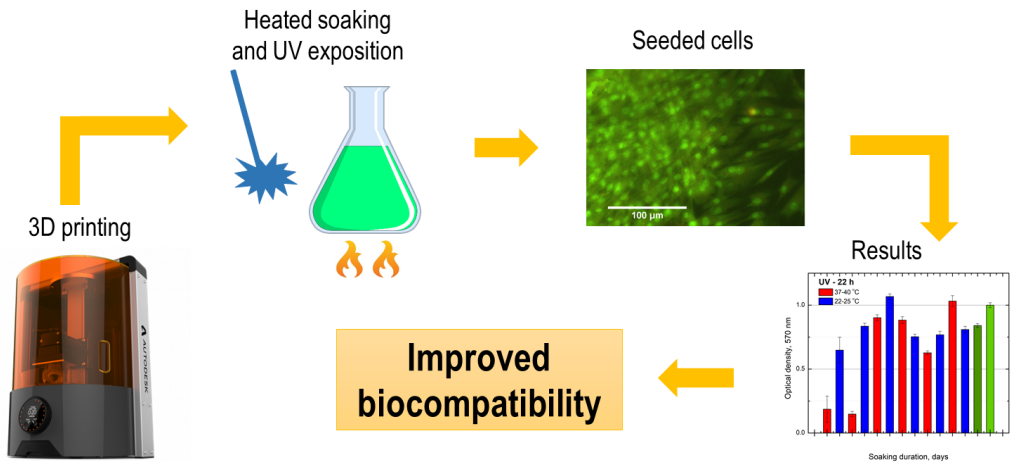


Figure 1. Steps of the experiment: first, samples are 3D printed; secondly, additional UV exposure and heated soaking is implemented; after that samples are seeded with cells and biocompatibility tests are made; finally, results are discussed and conclusions are made.

Statistical analysis was performed using R Studio by one-way analysis of variance (One-way ANOVA) with post-hoc Tukey HSD. Viability graphs were made with GraphPad Prism software. Data are represented as means and verified by at least 3 independent experiments. A value of $P < 0.05$ was considered to be statistically significant. The significant differences were stressed with symbols as shown in figures.

3. Results

In cell culture, myogenic stem cells assume spindle-shaped fibroblastic appearance, rapidly proliferate and became confluent in less than one week of culture [21]. Recently, cell shape has emerged as determinant which controls cell proliferation, growth, physiology and adaption for specific functions [22]. The cells also change their morphology in response to the toxic stimuli. To assess whether 3D printed samples can affect cell shape, we examined morphological changes of cells grown on differently processed samples. Scanning electron microscopy (SEM) analysis confirmed (Figure 3) a typical spindle-shaped cell phenotype. Moreover, almost confluent cover of the surfaces tested was detected after 24 h post-seeding.

Next, cell viability was analyzed to assess overall cell response to the tested samples. Data showed that cell viability increased with increasing soaking time. An optimal time for samples

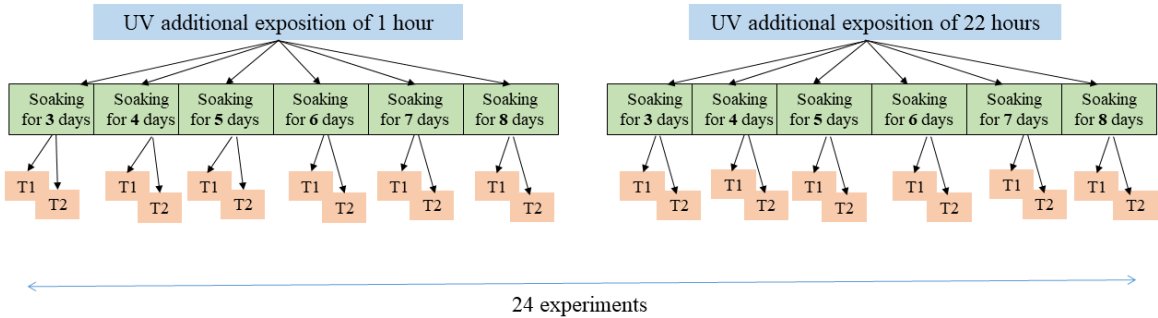


Figure 2. Experiments post-processing plan scheme, T1 - 22 – 25°C ; T2 - 37 – 40°C. First, polymerized structures were additionally UV exposed for 1 hour or 22 hours; after that samples were soaked in two different solvents for different duration from 1 to 8 days in two different temperatures.

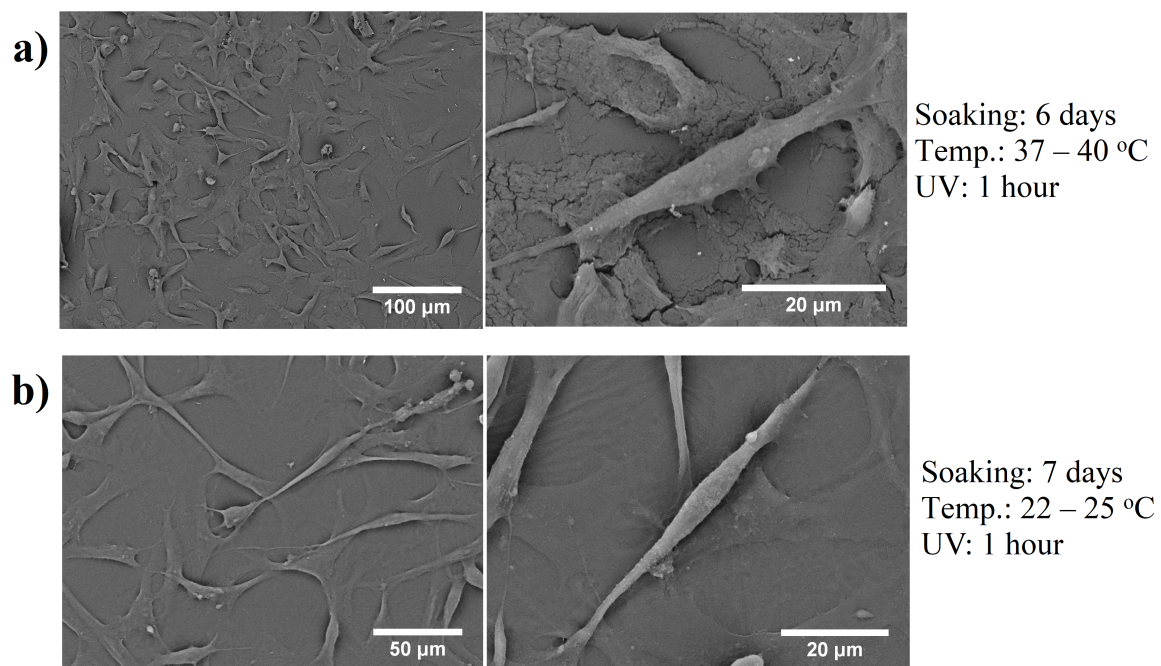


Figure 3. SEM analysis of seeded cells on different samples: a) soaking duration in heated isopropanol and methanol for 6 days; b) soaking duration in non-heated isopropanol and methanol for 7 days. It is noted, that the sample surfaces do not influence the morphology of the cells.

preparation in isopropanol and methanol is minimum 5 days. At day 7, there was reached the maximal biocompatibility. The effect of UV exposure was rather negligible. UV curing for 1 h increased cell viability 6–8 % and was comparable to control (Figure 4). However, the monomer cross-linking effect tend to be saturated, as the cell viability did not remarkably increase after longer (22 h) exposure time.

The samples had a modest effect on overall cell viability in post-processing dependent way. Therefore, a mode of cell death was evaluated subsequently (Figure 5). The higher number of dead cells detected in the population of cell grown on samples prepared at 37 – 40°C. We hypothesize that this phenomena can be determined by the material biodegradation under physiological temperature. However, our results show that this negative effect on cell viability may be reduced by the additional UV exposure with subsequent longer soaking in polar solvents. In all cases, necrosis was a dominant mode of cell death.

4. Discussion

Needless to say that modern trend of interdisciplinarity can lead to these results being relevant to not only 3D-bioprinting, but also as a supplement to other 3D printing techniques. Indeed, various combinations of additive-additive [9,23] and additive-subtractive [24,25] manufacturing techniques were used in the past to great effect. For instance, laser induced forward transfer (LIFT) [26] could be used to directly and selectively seed scaffolds with cells [9]. 3D femtosecond laser nanolithography could make sub-micrometer additions to the macro-structure of produced scaffolds [23], out of huge variety of different materials, including non-photosensitized [27,28] or functionalized [29] polymers. In essence, pairing of various processing techniques is a powerful way to offset most of the technological drawbacks and accentuate advantages [1,25]. For instance, 3D laser nanolithography is struggling to process elastic materials [14,30]. Thus, by pairing it to stereolithography would allow to make macro-level elastic structures that would require only minor laser made additions. Majority of currently used synthetic elastomers are reproducible, cost effective, and excellent alternatives to extracellular matrix. However, they have to meet high biocompatibility requirements. To enhance the biocompatibility of the materials used for the fabrication of tissue engineering scaffolds and

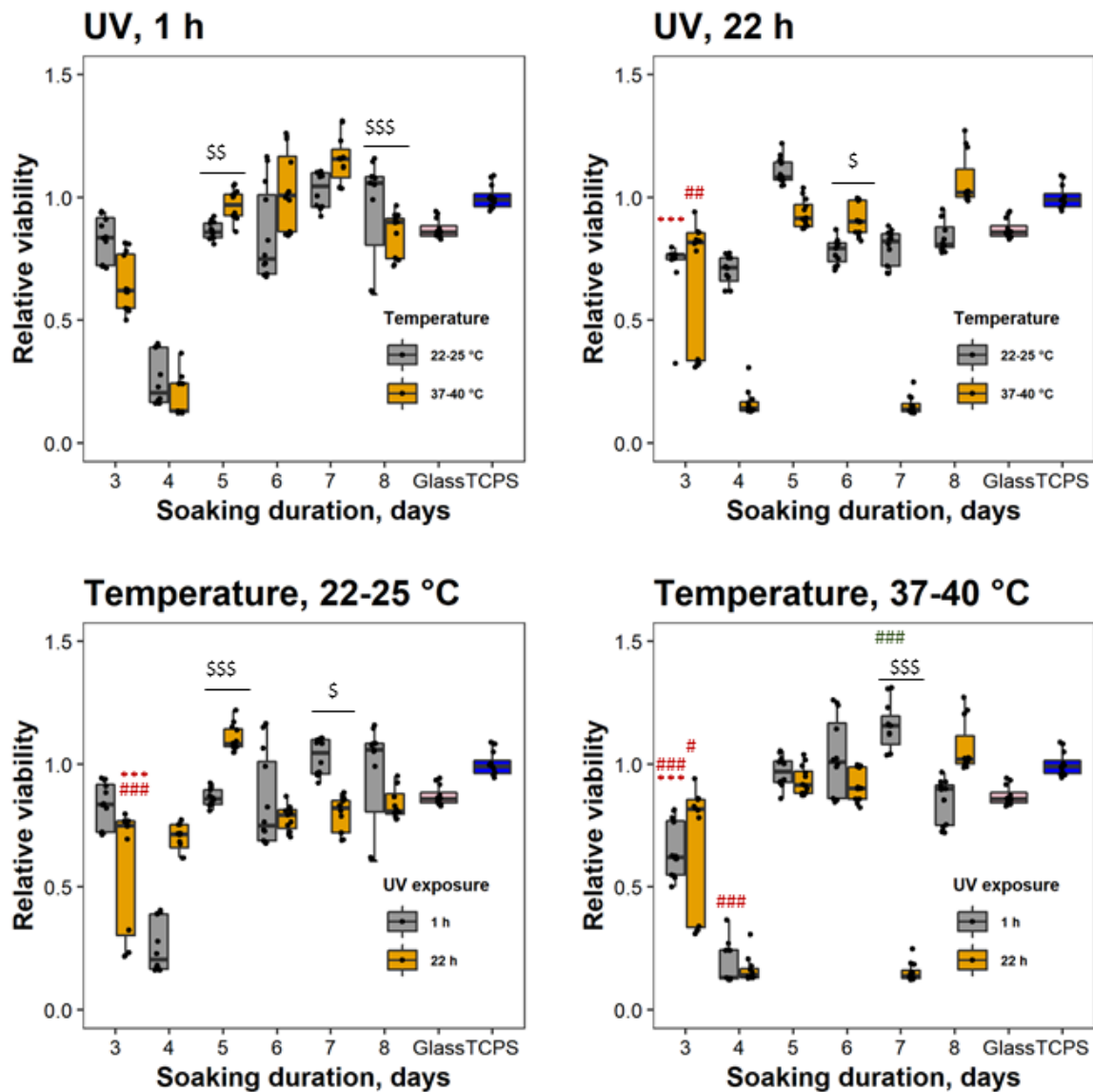


Figure 4. Biocompatibility test results. Figures above show relative viability depending on soaking duration and temperature, when UV exposition was 1 hour and 22 hours. Figures below show relative viability depending on soaking duration and UV exposition, when temperature was 22 – 25°C and 37 – 40°C. *, # - mark statistically significant changes then $p < 0.05$, ** - $p < 0.01$, *** - $p < 0.001$. * and # mark significant differences between tissue culture plate surface (TCPS) and glass surface, respectively. \$ marks significant differences between samples processed under the same time point. Red colour signifies differences below 1 (control level - TCPS), green colour - differences above 1.

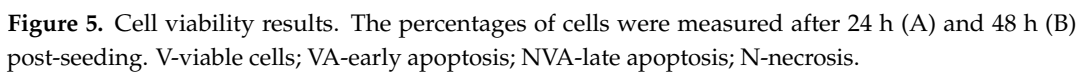


Figure 5. Cell viability results. The percentages of cells were measured after 24 h (A) and 48 h (B) post-seeding. V-viable cells; VA-early apoptosis; NVA-late apoptosis; N-necrosis.

other biomedical applications, surface modification strategies, such surface grafting, abrasive blasting and acid etching, surface coatings, heat and steam treatment were employed by several research groups [31]. These modifications alter surface roughness, hydrophilicity, surface charge, and has direct effect on biocompatibility and cell fate. Here we report more cost effective way to enhance elastomer biocompatibility which include prolonged soaking in polar solvents and additional UV exposure. Data suggest that proper exploitation of this procedure may quench the thirst of long-time unmet demands for biocompatibility.

5. Conclusions

In conclusion, a novel and straightforward protocol for improving the biocompatibility of 3D printed polymer objects (or coatings) was introduced and experimentally validated. The specific biocompatibility of commercial optically 3D printed elastomeric resin *Formlabs Flexible* surfaces using table-top *Ember* device was improved by implementation of additional UV exposure, heating and prolonged soaking in isopropanol and methanol. All samples did not have any remarkable effect on cellular morphology, yet the majority of the samples cell viability was higher than 85% (comparable to polystyrene substrates). What is more, a longer soaking duration, comparing 4 days (the sample of worst biocompatibility) and 7 days (the sample of best biocompatibility) tends to reveal more than 7 times higher biocompatibility test results. In brief, the table-top 3D printer fabricated and post-processed samples can be of high biocompatibility applying the proposed method due to higher polymerization degree and leaching out the non-polymerized monomers. The findings proposes the further application of such approach for all kind of polymer objects for basic cell studies and practical tissue engineering - not limiting to surfaces or coatings, but also free-form meshes and complex-shaped 3D scaffolds.

Author Contributions: Conceptualization, G.G. and M.M.; methodology, G.G., D.B. and M.M.; formal analysis, all authors; investigation, all authors; resources, D.B. and M.M.; data curation, G.G., D.B. and V.B.; writing—original draft preparation, all authors; writing—review and editing, G.G., D.B., and M.M.; supervision, D.B. and M.M.; project administration, D.B.; funding acquisition, D.B. and M.M.

Funding: This research was funded by the Research Council of Lithuania (Grant No. SEN-13/2015).

Conflicts of Interest: The authors declare no conflict of interest.

- Jonušauskas, L.; Juodkasis, S.; Malinauskas, M. Optical 3D printing: bridging the gaps in the mesoscale. *J. Opt.* **2018**, *20*, 053001.
- Schubert, C.; Langeveld, M.C.; Donoso, L.A. Innovations in 3D printing: a 3D overview from optics to organs. *Br. J. Ophthalmol.* **2014**, *98*, 159–161.
- Berman, B. 3-D printing: The new industrial revolution. *Bus. Horiz.* **2012**, *55*, 155–162.
- Auricchio, F.; Marconi, S. 3D printing: clinical applications in orthopaedics and traumatology. *EFORT Open Rev.* **2016**.
- Naftulin, J.S.; Kimchi, E.; Cash, S.S. Stramlined, Inexpensive 3D Printing of the Brain and Skull. *PLoS ONE* **2015**, *10*, e0136198.
- Dawood, A.; Marti, B.M.; Saurent-Jackson, V.; Darwood, A. 3D printing in dentistry. *BDJ* **2015**, *219*, 521–529.
- Melchels, F.P.W.; Feijen, J.; Grijpma, D.W. A review on stereolithography and its applications in biomedical engineering. *Biomaterials* **2010**, *31*, 6121–6130.
- Mačiulaitis, J.; Deveikytė, M.; Rekštytė, S.; Bratchikov, M.; Darinskas, A.; Šimbelytė, A.; Daunoras, G.; Laurinavičienė, A.; Laurinavičius, A.; Gudas, R.; Malinauskas, M.; Mačiulaitis, R. Preclinical study of SZ2080 material 3D microstructured scaffolds for cartilage tissue engineering made by femtosecond direct laser writing lithography. *Biofabrication* **2015**, *7*, 015015. doi:10.1088/1758-5090/7/1/015015.
- Ovsianikov, A.; Gruene, M.; Pflaum, M.; Koch, L.; Maiorana, F.; Wilhelmi, M.; Haverich, A.; Chichkov, B. Laser printing of cells into 3D scaffolds. *Biofabrication* **2010**, *2*, 014104.

10. Richter, B.; Hahn, V.; Bertels, S.; Claus, T.K.; Wegener, M.; Delaittre, G.; Barner-Kowollik, C.; Bastmeyer, M. Guiding Cell Attachment in 3D Microscaffolds Selectively Functionalized with Two Distinct Adhesion Proteins. *Adv. Mater.* **2017**, *29*.
11. Cao, Y.; Vacanti, J.P.; Paige, K.T.; Upton, J.; Vacanti, C.A. Transplantation of chondrocytes utilizing a polymer-cell construct to produce tissue-engineered cartilage in the shape of a human ear. *Plastic and reconstructive surgery* **1997**, *100*, 297–302.
12. Tappa, K.; Jammalamadaka, U. Novel Biomaterials Used in Medical 3D Printing Techniques. *J. Funct. Biomater.* **2018**, *9*(1).
13. Jammalamadaka, U.; Tappa, K. Recent Advances in Biomaterials for 3D Printing and Tissue Engineering. *J. Funct. Biomater.* **2018**, *9*(1).
14. Pashneh-Tala, S.; Owen, R.; Bahmaee, H.; Rekštytė, S.; Malinauskas, M.; Claeysens, F. Synthesis, Characterization and 3D Micro-Structuring via 2-Photon Polymerization of Poly(glycerol sebacate)-Methacrylate—An Elastomeric Degradable Polymer. *Front. Phys.* **2018**, *6*, 41.
15. Zhang, J.; Yang, B.; Li, H.; Fu, F.; Shi, X.; Dong, X.; Dai, M. A novel 3D-printed head phantom with anatomically realistic geometry and continuously varying skull resistivity distribution for electrical impedance tomography. *Sci. Rep.* **2017**, *7*, 4608.
16. Lin, N.J.; Bailey, L.O.; Becker, M.L.; Washburn, N.R.; Handerson, L.A. Macrophage response to methacrylate conversion using a gradient approach. *Acta Biomaterialia* **2007**, *3*, 163–173.
17. Ortega, I.; Deshpande, P.; Gill, A.A.; MacNeil, S.; Claeysens, F. Development of a microfabricated artificial limbus with micropockets for cell delivery to the cornea. *Biofabrication* **2013**, *5*(2).
18. Formlabs. Using Flexible Resin, <https://support.formlabs.com/s/article/Using-Flexible-Resin?www.formlabs.com> **2018**.
19. A.Zukauskas.; Matulaitiene, I.; Paipulas, D.; Niaura, G.; Malinauskas, M.; Gadonas, R. Tuning the refractive index in 3D direct laser writing lithography: towards GRIN microoptics. *Laser Photon. Rev.* **2015**, *9*(6), 706–712.
20. Mercille, S.; Massie, B. Induction of apoptosis in oxygen-deprived cultures of hybridoma cells. *Cytotechnology* **1994**, *15*, 117–128.
21. J.Zou.; Yuan, C.; Wu, C.; Cao, C.; Shi, Q.; Yang, H. Isolation and osteogenic differentiation of skeletal muscle-derived stem cells for bone tissue engineering. *Molecular Medicine Reports* **2014**, *9*(1).
22. Hart, M.L.; Lauer, J.C.; Selig, M.; Hanak, M.; Walters, B.; Rolauffs, B. Shaping the Cell and the Future: Recent Advancements in Biophysical Aspects Relevant to Regenerative Medicine. *J. Funct. Morphol. Kinesiol.* **2018**, *3*(2).
23. Jonušauskas, L.; Skliutas, E.; Butkus, S.; Malinauskas, M. Custom on demand 3D printing of functional microstructures. *Lith. J. Phys.* **2015**, *55*, 227–236. doi:10.3952/physics.v55i3.3151.
24. Amato, L.; Gu, Y.; Bellini, N.; Eaton, S.M.; Cerullo, G.; Osellame, R. Integrated three-dimensional filter separates nanoscale from microscale elements in a microfluidic chip. *Lab Chip* **2012**, *12*, 1135–1142. doi:10.1039/c2lc21116e.
25. Jonušauskas, L.; Rekštytė, S.; Buividas, R.; Butkus, S.; Gadonas, R.; Juodkasis, S.; Malinauskas, M. Hybrid Subtractive-Additive-Welding Microfabrication for Lab-on-Chip (LOC) Applications via Single Amplified Femtosecond Laser Source. *Opt. Eng.* **2017**, *56*, 094108.
26. Baseman, R.J.; Gupta, A.; Sausa, R.C.; Progler, C. Laser induced forward transfer. *Mater. Res. Soc. Symp. Proc.* **1987**, *101*.
27. Maximova, K.; Wang, X.; Balčytis, A.; Fan, L.; Li, J.; Juodkasis, S. Silk patterns made by direct femtosecond laser writing. *Biomicrofluidics* **2016**, *10*, 054101. doi:10.1063/1.4962294.
28. Jonušauskas, L.; Gailevičius, D.; Mikoliūnaitė, L.; Sakalauskas, D.; Šakirzanovas, S.; Juodkasis, S.; Malinauskas, M. Optically Clear and Resilient Free-Form μ -Optics 3D-Printed via Ultrafast Laser Lithography. *Materials* **2017**, *10*, 12. doi:10.3390/ma10010012.
29. Jonušauskas, L.; Lau, M.; Gruber, P.; Gokce, B.; Barcikowski, S.; Malinauskas, M.; Ovsianikov, A. Plasmon assisted 3D microstructuring of gold nanoparticle-doped polymers. *Nanotechnology* **2016**, *27*, 154001. doi:10.1088/0957-4484/27/15/154001.
30. Buividas, R.; Rekštytė, S.; Malinauskas, M.; Juodkasis, S. Nano-groove and 3D fabrication by controlled avalanche using femtosecond laser pulses. *Opt. Mater. Express* **2013**, *3*, 1674–1686.

- 221 31. John, A.A.; Subramanian, A.P.; Vellayappan, M.V.; ana S. K. Jaganathan, A.B.; Mohandas, H.;
222 Paramalinggam, T.; Supriyanto, E.; Yusofa, M. Review: physico-chemical modification as a versatile
223 strategy for the biocompatibility enhancement of biomaterials. *RSC Advances* **2015**, *5*.